

Article

Optimal Social and Vaccination Control in the SVIR Epidemic Model

Alessandro Ramponi * and Maria Elisabetta Tessitore

Department of Economics and Finance, University of Rome Tor Vergata, Via Columbia 2, 00133 Rome, Italy; tessitore@economia.uniroma2.it

* Correspondence: alessandro.ramponi@uniroma2.it

Abstract: In this paper, we introduce an approach to the management of infectious disease diffusion through the formulation of a controlled compartmental SVIR (susceptible–vaccinated–infected–recovered) model. We consider a cost functional encompassing three distinct yet interconnected dimensions: the social cost, the disease cost, and the vaccination cost. The proposed model addresses the pressing need for optimized strategies in disease containment, incorporating both social control measures and vaccination campaigns. Through the utilization of advanced control theory, we identify optimal control strategies that mitigate disease proliferation while considering the inherent trade-offs among social interventions and vaccination efforts. Finally, we present the results from a simulation-based study employing a numerical implementation of the optimally controlled system through the forward–backward sweep algorithm. The baseline model considered incorporates parameters representative of typical values observed during the recent pandemic outbreak.

Keywords: optimal control; economics; SVIR epidemic model

MSC: 93C15; 49K15; 49M05; 92D30



Citation: Ramponi, A.; Tessitore, M.E. Optimal Social and Vaccination Control in the SVIR Epidemic Model. *Mathematics* **2024**, *12*, 933. <https://doi.org/10.3390/math12070933>

Academic Editors: Wangjian Zhang, Zhicheng Du and Ziqiang Lin

Received: 19 February 2024

Revised: 11 March 2024

Accepted: 20 March 2024

Published: 22 March 2024



Copyright: © 2024 by the authors. Licensee MDPI, Basel, Switzerland. This article is an open access article distributed under the terms and conditions of the Creative Commons Attribution (CC BY) license (<https://creativecommons.org/licenses/by/4.0/>).

1. Introduction

Recently, numerous disease outbreaks have raised concerns about global public health. Avian influenza, Marburg virus, measles, Lassa fever, and other infectious diseases have highlighted their potential dangers. Organizations like the World Health Organization (WHO) have been at the forefront of monitoring and responding to these outbreaks, recognizing the urgent need for effective disease control strategies.

In the wake of the COVID-19 pandemic, the significance of robust response measures has been underscored. The European Centre for Disease Prevention and Control has outlined critical lessons learned in their technical report titled “Lessons from the COVID-19 pandemic” (<https://www.ecdc.europa.eu/en/publications-data/lessons-covid-19-pandemic-may-2023>, accessed on 21 June 2023). The report identifies four critical components of the response to health threats, emphasizing the pivotal role of analyzing epidemiological data and employing epidemiological modeling to inform decision-making.

Mathematical modeling remains a crucial factor in epidemiology, offering a more profound understanding of the fundamental mechanisms behind the propagation of newly emerging and resurgent infectious diseases and proposing effective strategies for their control. In such a framework, compartmental models, which originated with the Kermack and McKendrick (1927) [1] susceptible–infectious–recovered (SIR) model and have since undergone extensive development (see, e.g., the book by Brauer and Castillo-Chavez 2010 [2]), represent a recognized and established class of dynamic models used to depict the progression of infectious diseases. To recall qualitative theory on compartmental systems see [3]. Within this context, and focusing on the problem of disease containment, we regard two main tools for its control: implementing a set of social restrictions (e.g., lockdown periods) and deploying vaccination campaigns. The explicit introduction of a

vaccination compartment has been proposed by Liu et al. (2008) [4], which considers a modified version of the SIR model, named SVIR, in which the new compartment V is added, where the vaccines will belong before reaching immunity and, therefore, the recovered individuals.

Notably, while the adoption of stringent lockdown measures and the availability of a vaccine promise to curb the spread of the virus, they raise significant concerns regarding their pronounced economic impact, thereby elevating government decision-making to a multifaceted challenge. The optimal control theory of compartmental models offers a solid theoretical framework to capture essential aspects of optimal disease control policies. By representing the population as distinct compartments and modeling the dynamics of disease transmission, optimal control theory provides a systematic approach to determining the most effective strategies for disease control. This framework enables the exploration of various control measures and their impact on disease spread. It allows policymakers to optimize interventions based on desired objectives, such as minimizing infection rates, reducing economic costs, or maximizing resource utilization.

The literature on infectious disease analyzed via optimal control (see, e.g., Lenhart and Workman 2007 [5]) is experiencing rapid and extraordinary development. In such a context, Behncke (2000) [6] represents one of the early endeavors to incorporate a control methodology systematically. In preceding decades, research primarily concentrated on selective isolation and immunization strategies. Abakuks (1973) [7] explored the optimal separation of an infected population under the assumption of instantaneous isolation, while Hethcote and Waltman (1973) [8] introduced optimal vaccination strategies in their work. In more recent studies, Ledzewicz and Schattler (2011) [9] addressed an optimal control problem within a model incorporating vaccines and treatments in a dynamically expanding population. In a related vein, Gaff and Schaefer (2009) [10] conducted research encompassing SIR/SEIR/SIRS models, focusing on control parameters that govern vaccination rates, treatments provided to infected individuals, and the potential for quarantine measures to be applied as well. Bolzoni et al. (2017) [11] examined time-optimal control problems concerning the utilization of vaccination, isolation, and culling strategies within a linear framework. In the work of Miclo et al. (2020) [12], the researchers investigated a deterministic SIR model wherein a social planner exercised control over the transmission rate. This control aimed to mitigate the transmission rate's natural levels to prevent an undue strain on the healthcare system. Kruse and Strack (2020), as detailed in [13], expanded the SIR model to include a parameter subject to the planner's control, influencing disease transmission rates. This parameterization captured political measures such as social distancing and business lockdowns, which, while effective in curtailing disease transmission, often incurred substantial economic and societal costs. This trade-off was modeled by introducing convex cost functions related to the number of infected individuals and reductions in transmission rates. Similarly, in work by La Torre et al. (2021) [14], the objective of the social planner is to minimize the societal costs linked to the degrees of disease prevalence and the output foregone as a consequence of the implementation of social distancing measures, within a macroeconomic–epidemiological setup. Addressing the complex issue of epidemic management, Federico and Ferrari (2021) [15] focused on the endeavors of a policymaker to curtail the epidemic's spread while concurrently minimizing the associated societal costs within a stochastic extension of the SIR model. In Alvarez et al. [16], the authors study the optimal lockdown strategy for a planner who wants to control the fatalities of COVID-19, and minimize the cost of the lockdown. Concurrently, Federico et al. (2024) [17] investigated an optimal vaccination strategy utilizing a dynamic programming approach within a SIRS compartmental model. Calvia et al. (2024) [18] delved into controlling epidemic diffusion through lockdown policies within a SIRD model, employing a dynamic programming framework for in-depth analysis. In Chen et al. (2022) [19], a similar compartmental model is employed to investigate the impact of social distancing measures on mitigating COVID-19, examining the situation from both economic and healthcare standpoints. The study utilizes daily pandemic data, including figures for infected, recovered, and deceased

individuals and economic indicators such as mobility and financial market instability indices. The overarching multi-objective is to minimize the risks associated with disease transmission and economic volatility. Dasaratha (2023) in [20] analyzes the spread of a contagious disease when behavior responds to the disease's prevalence, while Al-Shbeil et al. (2023) [21] prove the disappearance of the pandemic, provided that an inequality involving the vaccination rate is satisfied.

Applying an optimal control framework to an SVIR dynamical model has received relatively limited attention within the existing literature. In the work of Ishikawa (2012) [22], the focus is directed toward a stochastic version of this model, where a thorough analysis of the corresponding stochastic optimal control problem revolves around the vaccination strategy, featuring a quadratic cost function. Witbooi et al. (2015) [23] extended the investigation, addressing deterministic and stochastic optimal control problems within the SVIR model framework. Their approach considers the vaccination rate a controllable parameter and integrates an additive cost function. Kumar and Srivastava (2017) [24] proposed and examined a control problem within this framework, incorporating both vaccination and treatment as control policies. Notably, they introduced a cost function linear in state variables, quadratic in treatment measures, and quartic in vaccination policies, respectively. Similarly, in the study by Garriga et al. (2022) [25], the deterministic optimal control problem is explored in a pandemic characterized by two distinct phases. During the initial phase, social restrictions serve as the sole viable containment measures for the disease, while at a subsequent random time, the availability of a vaccine is introduced. Optimal control strategies are thoroughly examined for both phases, utilizing one and two control variables. These analyses also specify the cost function's structural attributes by incorporating a utility function.

In this paper, we extend the results obtained in [26] by adding another dimension to the decision-making process. In our analysis, we postulate a scenario where a disease has already disseminated at an early stage, followed by a vaccine's availability. Hence, we employ an SVIR dynamic model to depict the transmission of an infectious disease, which two types of mitigation measures can influence within the purview of a social planner. These measures aim to curtail the rate of contagion within the population to decrease the impact of the disease. The central challenge lies in determining the optimal response by balancing the restrictions that minimize disease prevalence, the vaccination rate, and the economic costs associated with the strategy's implementation. To comprehensively account for the impact of these measures, differently from [23], we introduce an explicit cost function that distinctly factors in the expenses associated with handling the infected population, conducting vaccination campaigns, and the economic impact of social restrictions. By specifying the functional form of the cost functional, we can characterize the optimal control strategy function by applying Pontryagin's Maximum Principle, see, e.g., Lenhart and Workman (2007) [5].

The optimally controlled SVIR dynamic and the corresponding optimal policies are analyzed by implementing the forward–backward sweep algorithm, as described in Lenhart and Workman (2007) [5]. It is a two-step procedure that proved to be a practical approach to solving a wide range of optimal control problems by iteratively refining the control functions based on the state–costate variables, as established by the necessary conditions given by the maximum principle. The numerical simulations are conducted within two main epidemiological scenarios, characterized by different basic reproduction numbers, corresponding to disease-free and endemic equilibria of the dynamical model, respectively. The main results of our empirical analysis show the consistent reduction in total cost achieved by implementing the optimal policy, compared with the three benchmark strategies considered.

The paper is structured as follows. Section 2 introduces the SVIR dynamical model and the corresponding control problem, for which we characterize the functional form of the optimal control strategies. The quantitative analysis is reported in Section 3, which summarizes the results of the numerical simulations. In the final Section 4, we highlight our main findings and discuss directions for future research.

2. Problem Formulation

2.1. The SVIR Model

Liu et al. proposed the SVIR model in [4] to extend the well-known SIR model by adding a vaccination program (continuous or impulsive) for the population under study. The model consists of four groups: the susceptibles, S , the infected, I , the recovered, R , and the vaccinees, V , who started the vaccination process. The fractions of the total population in each group are denoted by S , V , R , and I , respectively. The model assumes that the disease is transmitted at a rate β when the susceptible individuals come into contact with the infected ones and that the infected individuals recover at a rate γ . The vaccinated individuals acquire immunity against the disease at a rate γ_1 , and they can also be infected at a reduced rate β_1 , which is lower than β because some immunity is gained after vaccination. The parameter α represents the rate at which the susceptible individuals join the vaccination program, and μ is the birth-death rate. Figure 1 illustrates how the population moves among the four compartments S , V , I , and R .

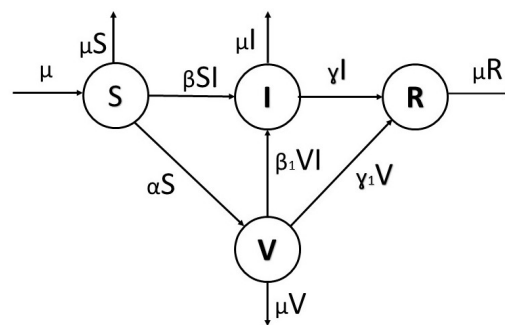


Figure 1. The basic SVIR model graph.

The following system of first-order differential equations captures the framework of the continuous vaccination process:

$$\begin{cases} \frac{dS}{dt}(t) = -\beta S(t)I(t) - \alpha S(t) + \mu - \mu S(t) & S(0) = S_0 \\ \frac{dV}{dt}(t) = \alpha S(t) - \beta_1 V(t)I(t) - \gamma_1 V(t) - \mu V(t) & V(0) = V_0 \\ \frac{dI}{dt}(t) = \beta S(t)I(t) + \beta_1 V(t)I(t) - \gamma I(t) - \mu I(t) & I(0) = I_0 \\ \frac{dR}{dt}(t) = \gamma_1 V(t) + \gamma I(t) - \mu R(t) & R(0) = R_0. \end{cases} \tag{1}$$

Let the parameters $\beta, \beta_1, \gamma, \gamma_1, \mu$ be positive real numbers and α be a non-negative real number. We also assume that the initial values S_0, V_0, I_0, R_0 are positive real numbers and their sum is equal to 1. These assumptions are made because model (1) describes human populations, and it can be proven that the solutions of the system remain non-negative if the initial values are non-negative, as shown in [4]. Furthermore, we note that if we define $N(t) = S(t) + V(t) + I(t) + R(t)$, then we can see from (1) that $\frac{dN}{dt}(t) = 0$; therefore, $N(t) = N_0 \equiv 1$, for all $t \geq 0$.

The state variable R does not appear in the first three equations of the system (1), so we can analyze the properties of the system using only the variables S , V , and I . As shown in [4], the SVIR model has a disease-free equilibrium E_0 (meaning an equilibrium $E_0 = (S^*, V^*, I^*)$ such that $I^* \equiv 0$), and an endemic equilibrium $E_+ = (S^+, V^+, I^+)$ with $I^+ > 0$. Furthermore, the basic reproduction number R_0^C determines its long-term behavior (see, e.g., [27]):

$$R_0^C = \frac{\mu\beta}{(\mu + \alpha)(\mu + \gamma)} + \frac{\alpha\mu\beta_1}{(\mu + \gamma_1)(\mu + \alpha)(\mu + \gamma)}, \tag{2}$$

and it is summarized in the two following theorems, which are proved in [4]:

Theorem 1. *If $R_0^C < 1$, then the disease-free equilibrium, E_0 , which always exists, is locally asymptotically stable and is unstable if $R_0^C > 1$. Moreover, $R_0^C > 1$ if and only if system (1) has a unique positive equilibrium, E_+ , and it is locally asymptotically stable when it exists.*

Theorem 2. *If $R_0^C \leq 1$, then the disease-free equilibrium, E_0 , is globally asymptotically stable. And if $R_0^C > 1$, the endemic equilibrium, E_+ , is globally asymptotically stable in all the regions of feasible model solutions, except for the constant solution identically equal to E_0 .*

2.2. The Optimal Control Problem

This section presents the controlled SVIR model and its related deterministic optimal control problem.

As in standard SVIR models, let S , V , I , and R represent susceptible, vaccinated, infected, and recovered, respectively. By S , V , I , and R , we denote the percentage of the total population belonging to each group.

We consider a vector control variable $u(\cdot) = (u_0(\cdot), u_1(\cdot))$. The component $u_0(\cdot)$ is meant to govern the social restrictions imposed by the social planner on a population until a specific time, T , which is the final time of government restriction, while the component $u_1(\cdot)$ is meant to govern the rate at which susceptible people are moving into the vaccinees compartment via the vaccination program. The birth and death rates are assumed to be the same and are denoted by μ .

The control variable $u = (u_0, u_1)$ belongs to the admissible set \mathcal{U} , defined as

$$\mathcal{U} = \{u : [0, T] \rightarrow [0, \bar{u}_0] \times [0, \bar{u}_1] : \text{Lebesgue measurable, } \bar{u}_0, \bar{u}_1 \in (0, 1]\}.$$

The control variable u_0 allows for the *adjustment* of the disease transmission rate. It captures the restrictions the social planner imposes to govern the speed at which the infection spreads, while ε quantifies the vaccine ineffectiveness (if $\varepsilon \equiv 0$, no vaccinated individual is infected). The goal is to create a scenario where the infection rate β is high without control ($u_0 = 0$), and low with increasing controls. The function $\beta(u_0)$ reflects both the infectiousness of the disease and the social planner’s measures to control the infection spread.

The control variable u_1 captures the cost of the vaccination, which we assume to be proportional to u_1S , being the flux of individuals from S to V or, equivalently, the number of newly vaccinated individuals in a unit of time. Furthermore, we set $\beta_1 = \varepsilon\beta$, where ε quantifies the vaccine ineffectiveness (if $\varepsilon \equiv 0$ no vaccinated individual is infected), and $0 \leq \varepsilon \leq 1$.

Thus, we have the following controlled SVIR model (see Figure 2):

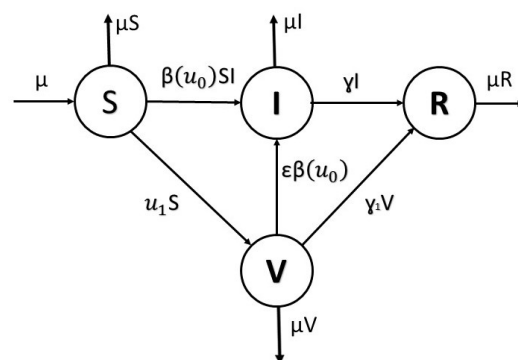


Figure 2. The controlled SVIR model graph.

$$\left\{ \begin{array}{l} \frac{dS}{dt}(t) = -\beta(u_0(t))S(t)I(t) - u_1(t)S(t) + \mu - \mu S(t) \quad S(0) = S_0 \\ \frac{dV}{dt}(t) = u_1(t)S(t) - \varepsilon\beta(u_0(t))V(t)I(t) - \gamma_1V(t) - \mu V(t) \quad V(0) = V_0 \\ \frac{dI}{dt}(t) = \beta(u_0(t))(t)S(t)I(t) + \varepsilon\beta(u_0(t))V(t)I(t) - \gamma I(t) - \mu I(t) \quad I(0) = I_0 \\ \frac{dR}{dt}(t) = \gamma_1V(t) + \gamma I(t) - \mu R(t) \quad R(0) = R_0, \end{array} \right. \quad (3)$$

where we assume that the initial data $S_0, V_0, I_0, R_0 \in \mathbb{R}^+$, and $S_0 + V_0 + I_0 + R_0 = 1$. The above assumptions are stated since model (3) represents human populations, and it can be shown that the solutions of the system are non-negative given non-negative initial values; see [4]. As before, we immediately have from (3) that $\frac{dN}{dt}(t) = 0$: hence $N(t) = N_0 \equiv 1$, for all $t \geq 0$.

Since the recovered people, R , do not appear in the first three equations of (3) or in the costs of the disease, we consider the following system:

$$\left\{ \begin{array}{l} \frac{dS}{dt}(t) = -\beta(u_0(t))(t)S(t)I(t) - u_1(t)S(t) + \mu - \mu S(t) \quad S(0) = S_0 \\ \frac{dV}{dt}(t) = u_1(t)S(t) - \varepsilon\beta(u_0(t))V(t)I(t) - \gamma_1V(t) - \mu V(t) \quad V(0) = V_0 \\ \frac{dI}{dt}(t) = \beta(u_0(t))(t)S(t)I(t) + \varepsilon\beta(u_0(t))V(t)I(t) - \gamma I(t) - \mu I(t) \quad I(0) = I_0. \end{array} \right. \quad (4)$$

To specify the control problem, we must define a functional to quantify the cost of spreading the disease. Specifically, we consider the costs due to infection and those attributable to vaccination, with the latter assumed to be proportional to u_1^2S , the rate of individuals moving from S to V or, equivalently, the number of newly vaccinated people per unit of time. We categorize these expenses as comprising hospitalization costs for both inpatients, whether or not they require intensive care unit (ICU) services, and logistical expenditures associated with the vaccination program, such as setting up and operating a vaccination hub, along with its medical staff, among other components. We finally include the cost of social restrictions in our framework, which we assume to be a function, c , of the control, u_0 , such that c is strictly increasing and convex in u_0 , and that $c(0) = 0$. This implies that, without control, the total costs of the disease spread are due to the infection and the vaccination. By assuming an additive structure for the cost functional, we separate the costs solely due to the disease from those due to the “restrictions” imposed on society. Parameters $c_1, c_2 \in \mathbb{R}^+$ represent the infection cost and the vaccination cost, respectively.

Hence, the objective function is given by $J : \mathcal{U} \rightarrow \mathbb{R}$ such that

$$J(u_0, u_1) = \int_0^T [c(u_0(t)) + c_1I(t) + c_2u_1^2(t)S(t)]dt. \quad (5)$$

The aim is to find the best strategy, $u^* \in U$, and the related state variables, S^*, V^* and R^* , which minimize (5),

$$\min_{u \in \mathcal{U}} J(u) \quad \text{subject to (4).}$$

To prove the existence of such a strategy, u^* , we refer to [5,24,26,28].

Theorem 3. Let $\beta(\cdot)$ be a linear decreasing function and let $c(\cdot)$ be a strictly convex, twice continuous differentiable function, such that $c' > 0$ and $c(0) = 0$.

Then an optimal solution, u^* , for problems (4) and (5) exists, i.e., there exists an optimal control, $u^* \in \mathcal{U}$, such that $J(u^*) = \min J(u)$.

Proof. First of all, notice that the right-hand side functions of system (4) are Lipschitz continuous with respect to the state variables; hence, the Picard–Lindelöf theorem ensures that there exist solutions to (4). By definition, the set $[0, \bar{u}_0] \times [0, \bar{u}_1]$ is compact and convex, and since the system (4) is linear in the control variable, u , the result follows from applying Theorem 4.1 and Corollary 4.1 pp. 68–69 in [28]. □

Remark 1. By choosing a continuous, convex function $C(u, I, S)$ on $[0, \bar{u}_0] \times [0, \bar{u}_1]$ in (5), we can obtain a similar result as in Corollary 4.1 pp. 68–69 of [28]. We use $C(u, I, S) = c(u_0(t)) + c_1 I(t) + c_2 u_1^2(t) S(t)$ to separate the costs of social restrictions, infections, and vaccinations. This also allows us to solve the problem numerically.

We use the control theory in [28] or [5] to solve the optimal control problem. We define the Hamiltonian function, H , and the co-state variables, $\lambda_1(t)$, $\lambda_2(t)$, and $\lambda_3(t)$. We drop the time dependence of the state variables S, V, I , the control variables u_0, u_1 , and the co-state variables, unless stated otherwise. The Hamiltonian function of (4) and (5) is given by the following:

$$\begin{aligned}
 H(t, S, V, I, u_0, u_1, \lambda_1, \lambda_2, \lambda_3) &= c(u_0(t)) + c_1 I + c_2 u_1^2 S + \lambda_1 [-\beta(u_0)SI - u_1 S + \mu - \mu S] \\
 &+ \lambda_2 [u_1 S - \varepsilon \beta(u_0)VI - \gamma_1 V - \mu V] + \lambda_3 [\beta(u_0)SI + \varepsilon \beta(u_0)VI - \gamma I - \mu I].
 \end{aligned}
 \tag{6}$$

Theorem 4. Let (S^*, V^*, I^*, u^*) be an optimal solution for problems (4) and (5), then there exist adjoint functions, λ_1, λ_2 and λ_3 , satisfying the following system of differential equations:

$$\begin{cases}
 \lambda'_1 = [\beta(u_0^*)I^* + u_1^* + \mu]\lambda_1 - u_1^* \lambda_2 - \beta(u_0^*)I^* \lambda_3 - c_2 u_1^{2*} \\
 \lambda'_2 = [\varepsilon \beta(u_0^*)I^* + \gamma_1 + \mu]\lambda_2 - \varepsilon \beta(u_0^*)I^* \lambda_3 \\
 \lambda'_3 = \beta(u_0^*)S \lambda_1 + \varepsilon \beta(u_0^*)V^* \lambda_2 - u_1^* \lambda_2 - [\beta(u_0^*)S^* + \varepsilon \beta(u_0^*)V^* - \gamma - \mu]\lambda_3 - c_1,
 \end{cases}
 \tag{7}$$

with the transversality conditions on the co-states λ_1, λ_2 and λ_3 given by the following:

$$\lambda_1(T) = 0, \quad \lambda_2(T) = 0, \quad \lambda_3(T) = 0.$$

The optimal restriction policy u^* is such that

$$u^*(t) \in \operatorname{argmin}_{u \in [0,1] \times [0,1]} H(t, S^*, V^*, I^*, u, \lambda_1, \lambda_2, \lambda_3).
 \tag{8}$$

Proof. Suppose (S^*, V^*, I^*, u^*) is an optimal solution of (4) and (5). By Pontryagin’s maximum principle, the co-state variables λ_1, λ_2 , and λ_3 satisfy (7), which is derived from the partial derivatives of H in (6) with respect to S, V, I .

$$\begin{cases}
 \lambda'_1 = -\frac{\partial H}{\partial S} \\
 \lambda'_2 = -\frac{\partial H}{\partial V} \\
 \lambda'_3 = -\frac{\partial H}{\partial I},
 \end{cases}
 \tag{9}$$

with the transversality conditions $\lambda_1(T) = \lambda_2(T) = \lambda_3(T) = 0$.

The strict convexity, with respect to the control variable, u , of the Hamiltonian function, H , defined in (6), ensures the existence of a unique minimum; see [23]. Hence, we have the following:

$$u^*(t) \in \operatorname{argmin}_{u \in [0,1] \times [0,1]} H(t, S^*, V^*, I^*, u, \lambda_1, \lambda_2, \lambda_3). \quad \square$$

2.3. The Solution of a Class of Optimal Control Problems

We can make the result more specific by choosing a particular form for the transmission rate $\beta(u_0)$ and the cost function $c(u_0)$. For the former, we use a simple linear model, as follows:

$$\beta(u_0) = \beta_0(1 - u_0), \quad 0 \leq u_0 \leq 1. \tag{10}$$

We assume that $\beta_0 > 0$ is the specific rate at which the disease spreads. In this case, we model the scenario when the maximum control (i.e., $u_0 \equiv 1$) completely stops the disease from diffusing.

For the social cost function, $c(u_0)$, we choose the following specification for our practical application:

1. $c_{quad}(u_0) = bu_0^2, b > 0;$
2. $c_{exp}(u_0) = e^{ku_0} - 1, k > 0.$

We prove the following result that gives a full description of the optimal controls.

Proposition 1. *Let $\beta(u_0) = \beta_0(1 - u_0)$ and $c_{quad}(u_0) = bu_0^2$. Then the optimal control strategy $u_{quad}^* = (u_0^*, u_1^*)$ for problems (4)–(5) is given by the following:*

$$u_0^*(t) = \min \left\{ \max \left[0, \frac{\beta_0 I^*(t) [S^*(t)(\lambda_3(t) - \lambda_1(t)) + \varepsilon V^*(t)(\lambda_3(t) - \lambda_2(t))]}{2b} \right], \bar{u}_0 \right\}, \tag{11}$$

and

$$u_1^*(t) = \min \left\{ \max \left[0, \frac{\lambda_1(t) - \lambda_2(t)}{2c_2} \right], \bar{u}_1 \right\}. \tag{12}$$

Proof. In this case, the Hamiltonian function H is defined as follows:

$$H(t, S, V, I, u, \lambda_1, \lambda_2, \lambda_3) = bu_0^2 + c_1 I + c_2 u_1^2 S + \lambda_1 [-\beta_0(1 - u_0)SI - u_1 S + \mu - \mu S] + \tag{13}$$

$$+ \lambda_2 [u_1 S - \varepsilon \beta_0(1 - u_0)VI - \gamma_1 V - \mu V] + \lambda_3 [\beta_0(1 - u_0)SI + \varepsilon \beta_0(1 - u_0)VI - \gamma I - \mu I],$$

then, imposing first-order conditions to minimize the Hamiltonian, H , at S^*, I^*, V^*

$$\frac{\partial H}{\partial u_0} = 2bu_0 + I^* [\beta_0 S^* (\lambda_1 - \lambda_3) + \varepsilon \beta_0 V^* (\lambda_2 - \lambda_3)] = 0 \tag{14}$$

$$\frac{\partial H}{\partial u_1} = 2c_2 u_1 S - \lambda_1 S + \lambda_2 S = 0,$$

we derive the optimal restriction policy, $u_{quad}^* = (u_0^*, u_1^*)$. \square

Corollary 1. *Let $\beta(u_0) = \beta_0(1 - u_0)$ and $c_{quad}(u_0) = bu_0^2$.*

Then the optimal control strategy $u_{quad}^ = (u_0^*, u_1^*)$ for problems (4)–(5) satisfies*

$$\lim_{b \rightarrow +\infty} u_0^*(t) = 0 \quad \text{and} \quad \lim_{b \rightarrow 0} u_0^*(t) = \bar{u}_0$$

$$\lim_{c_2 \rightarrow +\infty} u_1^*(t) = 0 \quad \text{and} \quad \lim_{c_2 \rightarrow 0} u_1^*(t) = \bar{u}_1.$$

Proof. From the previous proposition, the dynamical system has bounded solutions for every $u \in \mathcal{U}$. By taking the limits in (11) and (12), we obtain the result. \square

We can find the solution for the exponential case in a similar way as we did for the quadratic case above.

Proposition 2. Let $\beta(u_0) = \beta_0(1 - u_0)$ and $c_{exp}(u_0) = e^{ku_0} - 1$.

If $\lambda_3(t) > \max\{\lambda_1(t), \lambda_2(t)\}$, then the optimal control strategy $u_{exp}^*(t) = (u_0^*, u_1^*)$ for problems (4)–(5) is given by

$$u_0^*(t) = \min \left\{ \max \left[0, \frac{1}{k} \ln \frac{\beta_0 I^*(t) K(t)}{k} \right], \bar{u}_0 \right\}, \tag{15}$$

and

$$u_1^*(t) = \min \left\{ \max \left[0, \frac{\lambda_1(t) - \lambda_2(t)}{2c_2} \right], \bar{u}_1 \right\}, \tag{16}$$

where $K(t)$ is defined as $K(t) = S^*(t)(\lambda_3(t) - \lambda_1(t)) + \epsilon V^*(t)(\lambda_3(t) - \lambda_2(t))$.

Remark 2. According to Pontryagin’s maximum principle, the optimal control is a function of three Lagrange multipliers: λ_1, λ_2 , and λ_3 . These multipliers correspond to the marginal cost of the susceptible population, the marginal cost of the vaccinated population, and the marginal cost of the infected population, respectively. Furthermore, the difference between λ_3 and λ_1 can be interpreted as the marginal cost of having an additional susceptible person become infected, while the difference between λ_3 and λ_2 can be interpreted as the marginal cost of having an additional vaccinated person become infected. Moreover, $\lambda_1 - \lambda_2$ represents the marginal cost of having an extra susceptible vaccinated person, thus referring to an individual who, even if vaccinated, can still be infected.

3. A Numerical Study

In this section, we present the results of a simulation study aimed at investigating the impact of an optimal control strategy on disease dynamics and the associated costs. This study aims to assess the effectiveness of various control measures in mitigating the spread of the disease and reducing the economic burden. We highlight that this section serves the purpose of presenting the outcomes of the proposed model without engaging in any empirical investigation. In particular, no attempt has been made to fit the SVIR model to actual data. It is important to note that while an empirical analysis of this nature would be significant, it exceeds the scope of the current paper and is therefore left for future research. We rely on applying the forward–backward sweep (FBS) algorithm to analyze the optimal control strategies in alternative settings. Such an algorithm effectively solves optimal control problems by iteratively refining the control function based on the state and costate variables; see [5]. It consists of two main steps. Firstly, the forward state Equations (4) are solved by utilizing an ordinary differential equation (ODE) solver. This step calculates the state variables using the current control function, $u_n(\cdot)$. Next, the costate Equations (7) are solved backward in time using the same ODE solver. These equations represent the adjoint variables that provide information about the sensitivity of the cost function concerning the state variables (see Remark 2). The control function is updated using the calculated state and costate variables based on the optimality conditions. This process generates a new approximation of the state, costate, and control $u_{n+1}(\cdot)$. These steps are repeated iteratively until a convergence criterion is satisfied, i.e., when the algorithm reaches an acceptable approximation of the optimal control function. See McAsey et al. (2012) [29] for a deep analysis of the convergence properties of the FBS method.

In the initial stage, we set up the algorithm by establishing the temporal discretization and determining the termination criterion. To be specific, we selected a fixed number of time points, N , uniformly distributed over the time interval $[0, T]$. The termination criterion was defined based on the non-decreasing behavior of the cost functional (5). Furthermore, we incorporated a technique of weighted averaging to update the solution iteratively. This

involved combining the new solution $u_{new}(\cdot)$ and the previous one $u_n(\cdot)$ in such a way that $u_{n+1}(\cdot) = u_{new}(\cdot)(1 - c^n) + u_n(\cdot)c^n$. In order to fine-tune the algorithm hyperparameters, we ran a set of preliminary experiments on our baseline model (see Table 1 and the description below) by changing the starting solution (no controls or full controls) and the smoothing parameter $c \in \mathcal{C}$, where $\mathcal{C} = \{c_i : c_i = c_{i-1} + \Delta c, c_0 = 0, i = 1, \dots, n + 1\}$. In our investigation, we found that a weighting constant value $c = 0.99$ provides the lowest minimum of the cost functional (5), and ensures the smoothing properties of the resulting solution. In contrast, no effect on the final optimal solution is observed concerning the starting point. The description of the implemented algorithm is given in the following Algorithm 1:

Table 1. Parameters for the baseline model.

Epidemiological/Dynamical Parameters			Economic Parameters		
Parameter	Value	Description	Parameter	Value	Description
β_0	0.220	transmission rate	b	0.4	quad. cost function
γ	0.0795	recovery rate from infected	k	0.0392	exp cost function
γ_1	0.0714	full immunization rate	c_1	1	infection cost
ϵ	0.078	vaccine ineffectiveness	c_2	0.02	vaccination cost
\bar{u}_0	1	maximum social control			
\bar{u}_1	0.006	maximum vaccination rate			
μ	2.5×10^{-5}	daily death rate			

Algorithm 1 Forward–backward sweep algorithm: Let $\underline{y}(t) = (S(t), I(t), R(t))$ and $\underline{u}(t) = (u_0(t), u_1(t))$. We denote here with $\dot{\underline{y}}(t) = F(\underline{y}(t), \underline{u}(t))$ and $\dot{\underline{\lambda}}(t) = G(\underline{\lambda}(t), \underline{y}(t), \underline{u}(t))$ the ODE systems (4) and (7), respectively. Furthermore, the optimality conditions are written as $\underline{u}^*(t) = H(\underline{y}^*(t), \underline{\lambda}^*(t))$ (see Formulas (11), (12) and (15), (16)).

Initialize: $\underline{u}^{(0)}(t)$ and $J_0 = J(\underline{u}^{(0)})$ ▷ see Formula (5)
repeat $n \geq 0$
 $\dot{\underline{y}}^{(n+1)}(t) = F(\underline{y}^{(n+1)}(t), \underline{u}^{(n)}(t)), \quad \underline{y}^{(n+1)}(0) = y_0$
 $\dot{\underline{\lambda}}^{(n+1)}(t) = G(\underline{\lambda}^{(n+1)}(t), \underline{y}^{(n+1)}(t), \underline{u}^{(n)}(t)), \quad \underline{\lambda}^{(n+1)}(T) = 0$
 $\underline{u}^{(new)}(t) = H(\underline{y}^{(n+1)}(t), \underline{\lambda}^{(n+1)}(t))$
 $\underline{u}^{(n+1)}(t) = (1 - c^n)\underline{u}^{(new)}(t) + c^n\underline{u}^{(n)}(t)$
until $J_{n+1} > J_n$

Now, we present the results for different instances of the controlled SVIR model, in order to show the main features of our modeling framework. The first model we consider, named the baseline model, is an extension of the one considered in [26].

3.1. Numerical Results: The Baseline Model, $R_0^C < 1$

To begin, we establish a set of fundamental epidemiological parameters for the simulations. The following parameters define the baseline model. We take our time unit to be a day. In particular, we set $\beta_0 = 0.22$, $\gamma = 0.0795$ and $\gamma_1 = 0.0714$ (implying $1/\gamma \approx 12.6$ and $1/\gamma_1 \approx 14$ days, respectively). The value of ϵ can be set by using an estimate of the vaccine effectiveness, VE , which is defined as the percentage reduction in the risk of disease among vaccinated persons relative to unvaccinated persons, implying $\epsilon \equiv (1 - VE)$. In our experiments, we used the value of VE as estimated for the three available vaccines for COVID-19 (see [30] (Table 3)), implying $\epsilon = 0.078$.

As introduced in Section 2.2, the cost functional (5) is given by the sum of three terms, each related to a specific aspect of the problem: the cumulative “social cost” $J_{SC}(u) = \int_0^T c(u_0(t))dt$, “infection cost” $J_{IC}(u) = \int_0^T c_1 I(t)dt$, and “vaccination cost” $J_{VC}(u) = \int_0^T c_2 u_1^2(t)S(t)dt$. We chose the corresponding weights by normalizing with respect to the infection cost in such a way that $c_1 = 1$ and $c_2 = 0.02$ (these values were obtained by using data from an empirical

investigation on the costs of the COVID-19 disease outlined in Marcellusi et al. [31], as described in Ramponi and Tessitore [26].)

In order to obtain comparable results among the cost models, we set the parameters $b = 0.04$, and $k = 0.03922$, respectively, so that, in the given time period, the value of the social cost with the maximum control $J_{SC}(\bar{u}_0)$ is about the same. In particular, as a result of a set of preliminary numerical experiments, as fully described in Ramponi and Tessitore (2023) [26] in the case of social control only, we found that by varying the social cost function parameter, it is possible to identify a regime in which the full-control strategy produces lower costs than the no-control strategy. As the parameter increases, the full-control strategy becomes increasingly costly, and at the same time, the optimal strategy “converges” to the no-control strategy.

In the framework of our baseline model, we consider three benchmark scenarios to compare with the optimal control. In the first scenario, the disease is neither controlled by social restrictions nor vaccinations (no-control/no-vax). This is the case where $u_0(\cdot) = u_1(\cdot) \equiv 0$. In the second scenario, we assume an uncontrolled SVIR model, i.e., $u_0(\cdot) \equiv 0$, and a vaccination campaign at the highest possible rate, \bar{u}_1 , $u_1(\cdot) \equiv \bar{u}_1$. The third scenario is built by assuming full social control, i.e., $u_0(\cdot) \equiv 1$, and $u_1(\cdot) \equiv \bar{u}_1$, as before. In particular, we assume that the healthcare system is able to vaccinate about 90% of the population in one year, which is $u_1(\cdot) \equiv \bar{u}_1 = 0.006$ (this means that $e^{-\bar{u}_1} \approx 0.1$). Regarding the starting conditions of the dynamic model, it is assumed that the infectious disease has been spreading in a population for a given period before containment measures are implemented and a vaccine is available. Hence, we set $I_0 = 0.04$, $V_0 = 0$, $R_0 = 0.12$, and $S_0 = 1 - I_0 - V_0 - R_0$.

The results of these experiments are reported in Figures 3–5, for the quadratic social cost functions. The qualitative behaviors of the optimal solutions for both social cost functions are very similar. In particular, in both instances, the optimal controls suggest maintaining the maximum control of the transmission rate for a few days and then reducing it progressively; concurrently, the vaccination campaign should be implemented at the highest possible rate for almost the entire period. In such a scenario, the total cost is reduced considerably compared with the three benchmark strategies, as shown in Tables 2 and 3, and the compartment dynamic is comparable with that of the benchmark with full control. Specifically, the observed peak in the compartment of infected individuals, under the absence of control measures, becomes entirely mitigated upon attaining the same population percentage within the compartment of recovered individuals, which is approximately 89.7%, compared with the value of 97.8% observed for the uncontrolled SVIR model. Moreover, the final percentage in the susceptible compartment is around 10% in the case of the optimal strategy (for the no-control/no-vax and full-control benchmarks), compared with 2% in the case of the uncontrolled SVIR model.

Table 2. Total costs, $J(u)$, of the strategies and the corresponding social, infection, and vaccination costs for the quadratic social cost function. In parentheses are the percentage value w.r.t. the total cost.

Contr. Strategy	$J(u)$	Social Cost	Infection Cost	Vaccination Cost
$u_0 \equiv 0, u_1 \equiv 0$	9.8731	0(0%)	9.8731(100%)	0(0%)
$u_0 \equiv 0, u_1 \equiv \bar{u}_1$	8.1198	0(0%)	8.1198(99.99%)	0.00001(0.0003%)
$u_0 \equiv 1, u_1 \equiv \bar{u}_1$	14.9033	14.4000(96.6226%)	0.5033(3.3768%)	0.0001(0.0006%)
u_0^*, u_1^*	2.5362	1.6369(64.5393%)	0.8993(35.4573%)	0.0001(0.0034%)

Table 3. Total costs, $J(u)$, of the strategies and the corresponding social, infection, and vaccination costs for the exponential social cost function. In parentheses are the percentage values w.r.t. the total costs.

Contr. Strategy	$J(u)$	Social Cost	Infection Cost	Vaccination Cost
$u_0 \equiv 0, u_1 \equiv 0$	9.8732	0(0%)	9.8732(100%)	0(0%)
$u_0 \equiv 0, u_1 \equiv \bar{u}_1$	8.1197	0(0%)	8.1197(99.99%)	0.00001(0.0003%)
$u_0 \equiv 1, u_1 \equiv \bar{u}_1$	14.9031	14.3997(96.6225%)	0.5033(3.3769%)	0.0001(0.0006%)
u_0^*, u_1^*	3.5498	2.6591(74.9073%)	0.8907(25.0903%)	0.0001(0.0024%)

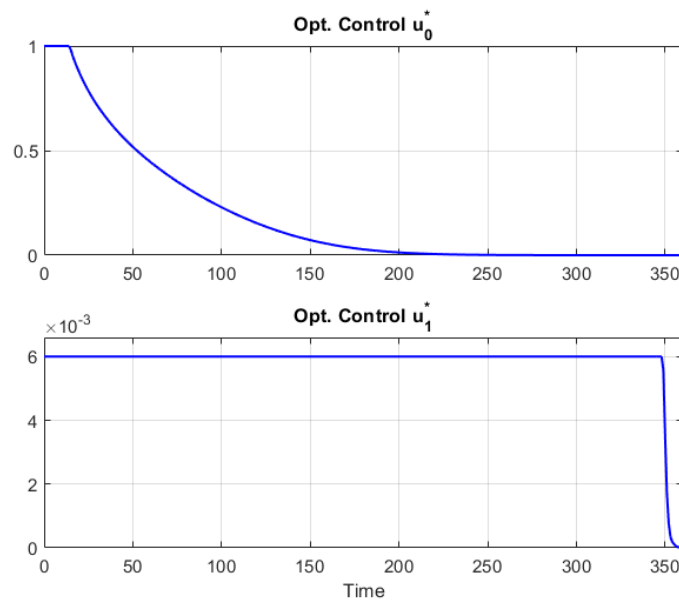


Figure 3. Optimal controls, u_0^*, u_1^* , for the baseline model with quadratic social cost function.

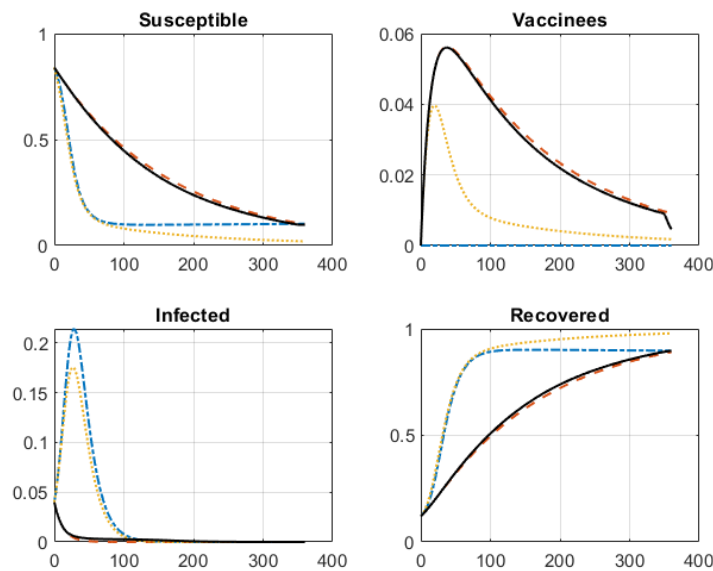


Figure 4. Compartmental dynamics corresponding to the uncontrolled/no-vax system ($u_0 = u_1 \equiv 0$, dash-dotted blue line), uncontrolled SVIR ($u_0 \equiv 0, u_1 \equiv \bar{u}_1$, dotted yellow line), fully controlled system ($u_0 \equiv 1, u_1 \equiv \bar{u}_1$, dashed red line), and optimally controlled system (u_0^*, u_1^* , black line), considered under a quadratic social cost function.

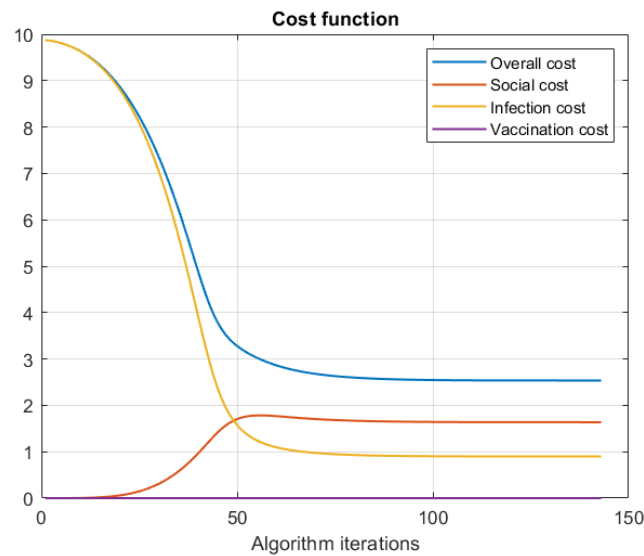


Figure 5. Cost function values along the FBS algorithm iterations, considered under a quadratic social cost function.

Sensitivity Analysis

The balance between cost factors that influence the function, J , affects the structure of the optimal solution. In particular, we analyzed the impact of the constraint, \bar{u}_1 , in relation to the cost of the vaccination, c_2 . As expected, when looking at the structure of the optimal control, $u_1^*(\cdot)$, as the value of c_2 decreases, with c_1 and the parameter b for the social cost function being fixed, the optimal control is "squeezed" toward the \bar{u}_1 constraint (see Figure 6).

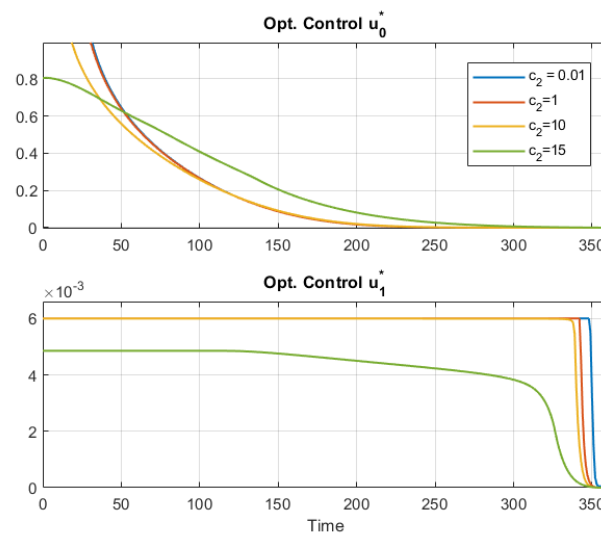


Figure 6. Optimal strategies for different values of the vaccination cost, c_2 .

3.2. Numerical Results: The Case $R_0^C > 1$

In this section, we consider a set of epidemiological parameters, implying a value of $R_0^C > 1$. As discussed in Section 2.1, such a condition implies the existence of an asymptotic equilibrium (S^+, V^+, I^+, R^+) of the uncontrolled dynamical system for which $I^+ > 0$. The parameters chosen in this scenario are reported in Table 4, and they imply a value of $R_0^C = 1.6261$. We set, as before, $\bar{u}_0 = 1$, and an (unrealistically) high value for $\bar{u}_1 = 0.8$, so that the optimizer could determine an optimal vaccination strategy unaffected by this constraint. The time (T) was set to 720 days.

Table 4. Parameters for the endemic equilibrium model.

Epidemiological/Dynamical Parameters			Economic Parameters		
Parameter	Value	Description	Parameter	Value	Description
β_0	0.4	transmission rate	b	0.12	quad. cost function
γ	0.002	recovery rate from infected	c_1	0.1	infection cost
γ_1	0.009	full immunization rate	c_2	1	vaccination cost
ϵ	0.4	vaccine ineffectiveness			
μ	2×10^{-4}	daily death rate			

Also, in this example, we can compare the behavior of the optimal system with benchmark models. In particular, we can observe how the susceptible compartment is quickly “emptied” due to a very high vaccination rate. On the other hand, the optimal strategy allows us to reduce the number of infected while increasing the recovered considerably, see Figure 7. In particular, the final values of infected and recovered compartments for the SVIR model are 24.14% and 75.47%, respectively, and 15.41% and 84.06% for the optimized model. At the same time, costs decrease significantly, as shown in Table 5.

The optimal strategy in this example (see Figure 8) sets the maximum social control in the initial period. This control gradually descends and simultaneously increases the optimal vaccination rate, which remains considerably high until it rapidly declines in the final period.

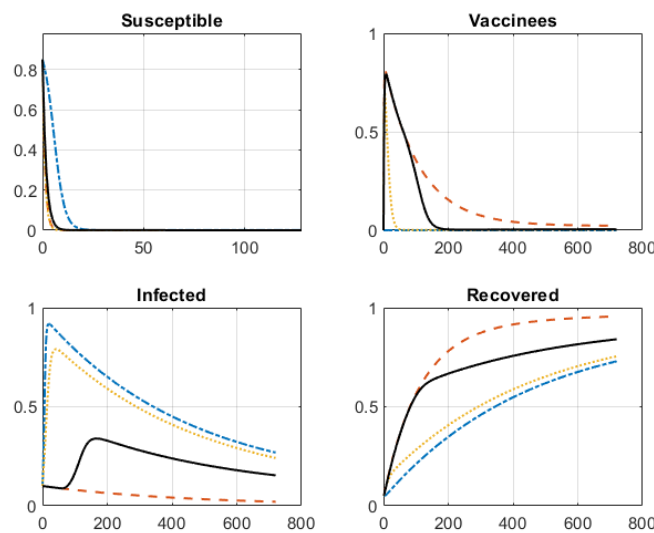


Figure 7. Compartmental dynamics corresponding to the uncontrolled/no-vax system ($u_0 = u_1 \equiv 0$, dash-dotted blue line), uncontrolled SVIR ($u_0 \equiv 0, u_1 \equiv \bar{u}_1$, dotted yellow line), fully controlled system ($u_0 \equiv 1, u_1 \equiv \bar{u}_1$, dashed red line), and optimally controlled system (u_0^*, u_1^* , black line), endemic equilibrium model.

Table 5. Total costs, $J(u)$, of the strategies and the corresponding social, infection, and vaccination costs for the endemic equilibrium model. In parentheses are the percentage values w.r.t. the total costs.

Contr. Strategy	$J(u)$	Social Cost	Infection Cost	Vaccination Cost
$u_0 \equiv 0, u_1 \equiv 0$	37.3778	0(0%)	37.3778(100%)	0(0%)
$u_0 \equiv 0, u_1 \equiv \bar{u}_1$	34.8572	0(0%)	33.3195(95.5886%)	1.5377(4.4114%)
$u_0 \equiv 1, u_1 \equiv \bar{u}_1$	91.6746	86.4000(94.2464%)	3.6129(3.9411%)	1.6617(1.8126%)
u_0^*, u_1^*	26.7954	9.8912(36.9137%)	15.7871(58.9170%)	1.1172(4.1694%)

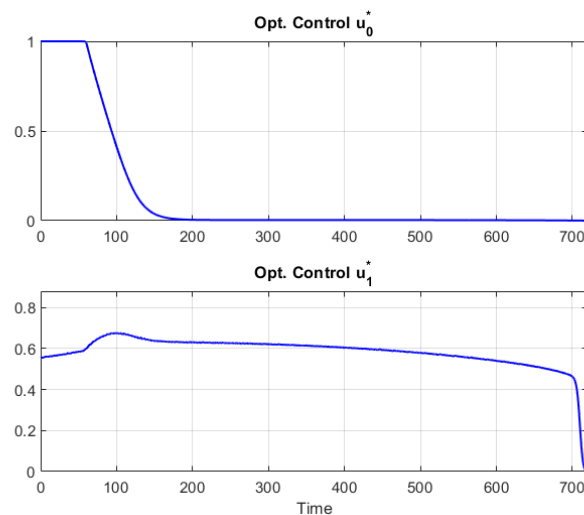


Figure 8. Optimal controls u_0^*, u_1^* for the endemic equilibrium model.

4. Conclusions

In this paper, we consider a controlled SVIR compartmental model used to characterize the dynamics of infectious diseases. This model aids in the development of a mathematical framework to analyze effective strategies for disease management, helping policymakers and public health authorities in their decision-making processes. The model incorporates two distinct control mechanisms: (i) social containment measures, encompassing a range of interventions such as lockdowns, curfews, school and university closures, and the cessation of commercial activities. These actions curb disease spread by lowering the transmission rate but come at the expense of a social cost. (ii) Vaccination campaign: The rate and efficiency of the vaccination campaign play a pivotal role in disease management. Vaccination reduces the spread of the disease and incurs its own cost.

We explicitly consider the cost of the disease as the sum of three distinct terms. (i) Social cost: arising from implementing social containment measures, including economic and societal disruptions. (ii) Infectious cost: encompassing the toll exacted by the disease in terms of morbidity, mortality, and healthcare burdens. (iii) Vaccination cost: reflecting the expenses incurred in the vaccination campaign. Using the Pontryagin maximum principle, under some conditions on the functional form of these costs, we could find the explicit structure of the optimal controls.

To assess the effectiveness of the proposed strategies, the optimally controlled system is simulated through the utilization of the forward–backward sweep algorithm. This simulation approach facilitates a deeper understanding of the dynamics of infectious diseases and allows for evaluating the proposed control measures in practical scenarios.

Our numerical experiment compares the system under the optimal strategy with three benchmark strategies: no controls/no vax, no social control/vax at the maximum rate, and maximum social control/maximum vax rate. In our simulation, we observe that, in the disease-free scenario ($R_C < 1$), the optimally controlled system significantly reduces the overall cost while keeping the final compartment values nearly identical to those of the fully controlled system. Conversely, the total cost is also reduced in the endemic scenario ($R_C > 1$). However, the final compartmental values fall between those achieved by the fully controlled system and those observed with other benchmark control strategies.

Finally, in future research, there is potential to explore various aspects of the SVIR compartmental model and its optimal control strategies. From an economic perspective, researchers may consider providing a more detailed description of the social cost function, which could involve investigating its relationship with financial and social indices and refining the characterization of infectious costs, including distinctions between costs related to hospitalization with or without ICU care. From a dynamic point of view, future studies

could expand the model by introducing additional compartments, such as “Quarantined” and “Dead”. Incorporating these compartments would lead to significant changes in the dynamics of the compartmental ODE system, providing new insights into the disease dynamics and control strategies. Finally, calibrating this family of models using observed data related to relevant epidemic phenomena, such as in the case of Al’os et al. [32] concerning the recent COVID-19 pandemic, presents a highly relevant and significant challenge.

Author Contributions: Both authors equally contributed to every aspect of the writing of this article. All authors have read and agreed to the published version of this manuscript.

Funding: This research received no external funding.

Data Availability Statement: The data presented in this study are available on request from the corresponding author.

Conflicts of Interest: The authors declare no conflicts of interest.

References

1. Kermack, W.O.; McKendrick, A.G. Contributions to the mathematical theory of epidemics. *Bull. Math. Biol.* **1991**, *53*, 33–55. [PubMed]
2. Brauer, F.; Castillo-Chavez, C. *Mathematical Models in Population Biology and Epidemiology*; Springer Science: Berlin, Germany, 2010.
3. Jacquez, J.A.; Simon, C.P. Qualitative Theory of Compartmental Systems. *Siam Rev.* **1993**, *35*, 43–79.
4. Liu, X.; Yasuhiro, T.; Shingo, I. SVIR epidemic models with vaccination strategies. *J. Theor. Biol.* **2008**, *253*, 1–11. [CrossRef]
5. Lenhart, S.; Workman, J.T. *Optimal Control Applied to Biological Models. Mathematical and Computational Biology Series*; Chapman & Hall/CRC: London, UK, 2007. [CrossRef] [PubMed]
6. Behncke, H. Optimal control of deterministic epidemics. *Optim. Control Appl. Methods* **2000**, *21*, 269–285.
7. Abakuks, A. An Optimal Isolation Policy for an Epidemic. *J. Appl. Probab.* **1973**, *10*, 247–262. [CrossRef]
8. Hethcote, H.W.; Waltman, P. Optimal Vaccination Schedules in a Deterministic Epidemic Model. *Math. Biosci.* **1973**, *18*, 365–381. [CrossRef]
9. Ledzewicz, U.; Schattler, H. On optimal singular controls for a general SIR-model with vaccination and treatment. *Conf. Publ.* **2011**, *2011*, 981–990. [CrossRef]
10. Gaff, H.; Schaefer, E. Optimal control applied to vaccination and treatment strategies for various epidemiological models. *Math. Biosci. Eng.* **2009**, *6*, 469–492.
11. Bolzoni, L.; Bonacini, E.; Soresina, C.; Groppi, M. Time-optimal control strategies in SIR epidemic models. *Math. Biosci.* **2017**, *292*, 86–96.
12. Miclo, L.; Spiroz, D.; Weibull, J. Optimal Epidemic Suppression under an ICU Constraint. *arXiv* **2020**, arXiv:2005.01327. [CrossRef]
13. Kruse, T.; Strack, P. Optimal Control of an Epidemic through Social Distancing. 2020. Available online: <https://ssrn.com/abstract=3581295> (accessed on 20 May 2023).
14. La Torre, D.; Liuzzi, D.; Marsiglio, S. Epidemics and macroeconomic outcomes: Social distancing intensity and duration. *J. Math. Econ.* **2021**, *93*, 102473.
15. Federico, S.; Ferrari, G. Taming the spread of an epidemic by lockdown policies. *J. Math. Econ.* **2021**, *93*, 102453.
16. Alvarez, F.; Argente, D.; Lippi, F. A Simple Planning Problem for COVID-19 Lock-down, Testing, and Tracing. *Am. Econ. Rev. Insights* **2021**, *3*, 367–82. [CrossRef]
17. Federico, S.; Ferrari, G.; Torrente, M.L. Optimal vaccination in a SIRS epidemic model. *Econ. Theory* **2024**, *77*, 49–74. [CrossRef]
18. Calvia, A.; Gozzi, F.; Lippi, F.; Zanco, G. A Simple Planning Problem for COVID-19 Lockdown: A Dynamic Programming Approach. *Econ. Theory*, **2024**, *77*, 169–196. [CrossRef]
19. Chen, K.; Pun, C.S.; Wong, H.Y. Efficient social distancing during the COVID-19 pandemic: Integrating economic and public health considerations. *Eur. J. Oper. Res.* **2022**, *304*, 84–98. [CrossRef] [PubMed]
20. Dasaratha, K. Virus dynamics with behavioral responses. *J. Econ. Theory* **2023**, *214*, 105739. [CrossRef] [PubMed]
21. Al-Shbeil, I.; Djenina, N.; Jaradat, A.; Al-Husban, A.; Ouannas, A.; Grassi, G. A New COVID-19 Pandemic Model including the Compartment of Vaccinated Individuals: Global Stability of the Disease-Free Fixed Point. *Mathematics* **2023**, *11*, 576. [CrossRef] [PubMed]
22. Ishikawa, M. Stochastic optimal control of an sir epidemic model with vaccination. In Proceedings of the 43rd ISICIE International Symposium on Stochastic Systems Theory and its Applications, Shiga, Japan, 30–31 October 2012. [CrossRef] [PubMed]
23. Witbooi, P.J.; Muller, G.E.; Van Schalkwyk, G.J. Vaccination control in a stochastic SVIR epidemic model. *Comput. Math. Methods Med.* **2015**, *2015*, 271654. [CrossRef]
24. Kumar, A.; Srivastava, P.K. Vaccination and treatment as control interventions in an infectious disease model with their cost optimization. *Commun. Nonlinear Sci. Numer. Simul.* **2017**, *44*, 334–343. [CrossRef]
25. Garriga, C.; Manuelli, R.; Sanghi, S. Optimal management of an epidemic: Lockdown, vaccine and value of life. *J. Econ. Dyn. Control* **2022**, *140*, 104351. [CrossRef]

26. Ramponi, A.; Tessitore, M.E. The economic cost of social distancing during a pandemic: An optimal control approach in the SVIR model. *Decis. Econ. Financ.* **2023** <https://doi.org/10.1007/s10203-023-00406-0>.
27. Van den Driessche, P. Reproduction numbers of infectious disease models. *Infect. Dis. Model.* **2017**, *2*, 288–303. [[CrossRef](#)]
28. Fleming, W.H.; Rishel, R.W. *Deterministic and Stochastic Optimal Control, Applications of Mathematics*; Springer: New York, NY, USA; Heidelberg/Berlin, Germany, 1975; Volume 1. [[CrossRef](#)]
29. McAsey, M.; Mou, L.; Han, W. Convergence of the forward-backward sweep method in optimal control. *Comput. Optim. Appl.* **2012**, *53*, 207–226. [[CrossRef](#)]
30. Andrews, N.; Stowe, J.; Kirsebom, F.; Toffa, S.; Rickeard, T.; Gallagher, E.; Gower, C.; Kall, M.; Groves, N.; O’Connell, A.-M.; et al. COVID-19 Vaccine Effectiveness against the Omicron (B.1.1.529) Variant. *N. Engl. J. Med.* **2022**, *386*, 1532–1546. [[CrossRef](#)]
31. Marcellusi, A.; Fabiano, G.; Sciattella, P.; Andreoni, M.; Mennini, F.S. The Impact of COVID–19 Vaccination on the Italian Healthcare System: A Scenario Analysis. *Clin. Drug Investig.* **2022**, *42*, 237–242. [[CrossRef](#)] [[PubMed](#)]
32. Alós, E.; Mancino, M.E.; Merino, R.; Sanfelici, S. A fractional model for the COVID-19 pandemic: Application to Italian data. *Stoch. Anal. Appl.* **2020**, *39*, 842–860. <https://doi.org/10.1080/07362994.2020.1846563>.

Disclaimer/Publisher’s Note: The statements, opinions and data contained in all publications are solely those of the individual author(s) and contributor(s) and not of MDPI and/or the editor(s). MDPI and/or the editor(s) disclaim responsibility for any injury to people or property resulting from any ideas, methods, instructions or products referred to in the content.